

# Validation of hot ring rolling industrial process 3D simulation

Luca Giorleo · Claudio Giardini · Elisabetta Ceretti

Received: 12 April 2011 / Accepted: 10 June 2011  
© Springer-Verlag France 2011

**Abstract** Ring rolling is a hot forming process used in the production of railway tyres, anti friction bearing races and different ring shaped work pieces for automotive energy production and aerospace applications. The advantages of ring rolling process include short production time, uniform quality, closed tolerances, good material quality and considerable saving in material cost. Despite the benefits some problems still exist according to a correct selection of the process parameters. Due to the nature of the process different rolling mills (driving, idle and axial rolls) are involved and the correct selection of the process parameters is not so feasible. Moreover an experimental approach to solve this problem risks to be more expensive. Actually FE codes are available to simulate the non linear problem that characterizes a ring rolling process. In this work a FE model, based on Deform 3D software, was tested versus experimental results acquired from an industrial plant. The accuracy of the FE model was analyzed through a dual comparison: by geometrical and by physical aspects. A good agreement was found between experimental and numerical results for both comparisons and, as a consequence, this code could be used in order to investigate and optimize the process parameters that characterize the ring rolling process in a virtual not expensive environment. The validated model will allow the studies of more environment-friendly process configurations.

**Keywords** FE approach · Ring rolling · Experimental validation · Energy saving

## Introduction

Ring rolling is a hot forming process used for the production of ring shaped, seamless and cylindrical symmetry work pieces. The process and equipment are similar in principle to rolling mills used for plate production. Indeed in both processes the metal is rolled between two rolls which move toward each other to form a continuously reducing gap. In ring rolling, the rolls are of different diameters and geometries.

The ring rolling process is basically used in the production of railway tyres, anti friction bearing races and different ring shaped work pieces for automotive and aerospace applications. It could be an hot or cold process and different alloys as alloy steels, light alloys and titanium can be worked. The advantages of ring rolling process include short production time, uniform quality, close tolerances and considerable saving in material cost. This process, compared to others as casting or plasma cutting, could provide lower working temperature, less material required and consequently a reduction in energy consumption. Moreover the main advantage of the work pieces produced by ring rolling process, compared to other technological processes, is given by the size and orientation of grains, especially on the worked surface which give to the final product excellent mechanical properties [1]. In Fig. 1 the main production steps of the ring rolling process are summarized.

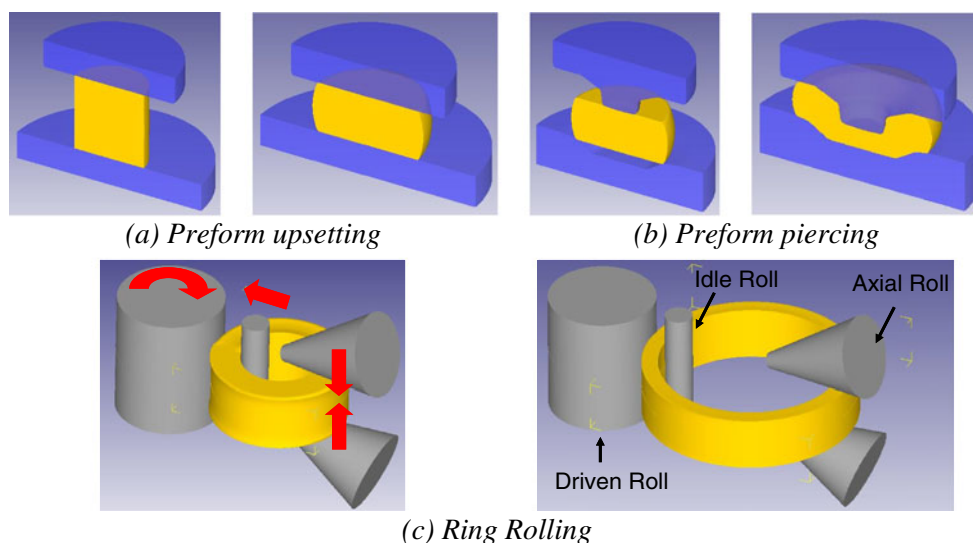
As reported in Fig. 1, the process begins with a forged bar that has been upset (a) and pierced (b) to obtain a hollow circular preform. The preform is placed over the idle

---

L. Giorleo (✉) · E. Ceretti  
Department of Mechanical and Industrial Engineering,  
University of Brescia,  
Brescia, Italy  
e-mail: luca.giorleo@ing.unibs.it

C. Giardini  
Department of Design and Technologies, University of Bergamo,  
Dalmine, Bergamo, Italy

**Fig. 1** Main characteristic of ring rolling. **a** Preform upsetting. **b** Preform piercing. **c** Ring rolling



roll, and it is forced toward the driven roll (c). At the same time, the axial rolls apply pressure in a direction parallel to the ring axis. So the idle roll reduces the width while the axial rolls reduce the height of the ring cross section. The coupled idle and axial rolls movements define the shape of the cross section and increase the ring diameter. The work piece starting sections could have a rectangular or complex shape. As it can be observed from Fig. 1, due to the nature of the process, different rolling mills (driven roll, idle and axial roll) are involved and the correct selection of the process parameters is not so feasible.

In literature, the first researches on this topic were based on experimental approaches [2–5] but, due to the dimensions of the mechanical parts involved into the process (a typical ring produced by this process can have a final diameter equal to 3 m and height equal to 0.5 m) it was very expensive. To save cost different approaches were followed focused on cold ring rolling process: some authors designed experiments considering a downscaling of rolled ring dimensions [6, 7] while others by changing ring material (i.e. wax) [8].

Meshless approaches are available to solve problems related to large plastic deformation; different authors utilized the meshless method in metal forming to perform simulations of basic two-dimensional metal forming processes including extrusion, rolling, upsetting and forging [9–11]. However the solutions obtained take into account many simplifications (i.e. no sliding occurred at the tool and work piece interface, no solution of strain rate and stress field). The meshless approach seems to be interesting but up to now many challenging topics need to be solved and there is a considerable lack of combined theoretical experimental research activities for assessing the accuracy and performance of meshless methods development.

Actually FE codes are available to simulate the non linear problem that characterizes ring rolling. It must be underlined

that, because of the complex nature of the process, in order to consider these software as reliable a comparison with experimental values is needful. In this work, a FE model, based on Deform 3D software, was tested versus experimental results acquired from an industrial plant. The accuracy of this FE model was analyzed based on a dual comparison by geometrical and by physical aspects. A good agreement was found between experimental and numerical results for both comparisons and so, this code could be used in order to investigate and optimize the process parameters that characterize the ring rolling process. This goal is only a starting point to optimize the ring rolling process. Once tested the FE accuracy, the following tasks will be the evaluation of roll (driven, idle and axial) feed laws and so milling curves that minimize the energy needed to ring rolled production. Moreover due to the FE technique will be, also, possible to evaluate different parameters that are difficult to measure by experimental approach (i.e. ring working temperature) in order to test different environment conditions that could increase the energy saving.

## FE modeling

Since 1968 ring rolling process was object of several scientific studies; following the years the process was analyzed using analytical methods such as the upper bound method [12] and the variation method of Hill [13]. Since 1988, the FE numerical approach was followed in order to simulate the ring rolling process. The method was quite accurate but require long computational time due to three main factors:

- the first is the unsteady state of the flow of the material, since the size of the ring section continuously changes, differently from standard flat rolling. So, the contact

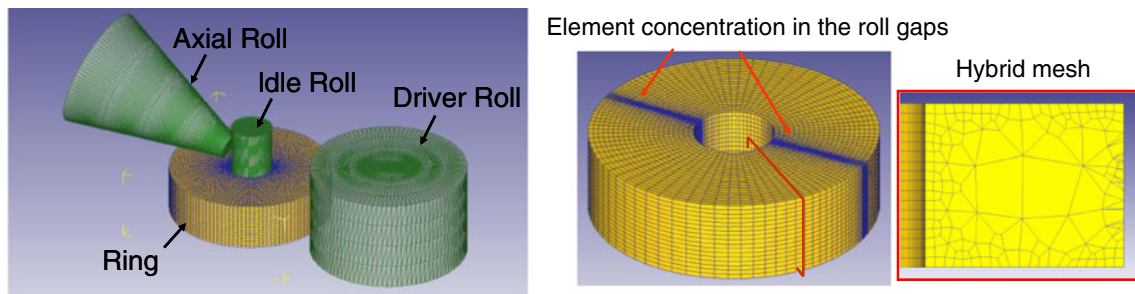


**Fig. 2** 3D-FE scheme model of the ring rolling process

conditions between ring and rolls continuously change. This leads to a significant increase of the computational time;

- the second factor is the high number of revolutions that a ring must do to obtain the desired shape. The direct consequence is that the number of elements required for finite element analysis is very high with respect to a standard deformation process (e.g. forging). For this reason, the computational time increases significantly;
- the third factor is the non-linearity of the relations that describe the flow curves of the material. For each simulation step, a linearization of algebraic systems is necessary, this causes a further increase of computational time.

Nowadays several authors focused their studies to simulate a hot ring rolling process: these works are based on the FE method and they follow different approaches. The main differences between these works concern the adopted mesh (hybrid or tetrad), the finite element method (rigid-plastic, elastic-plastic), the problem design (two-dimensional, three-dimensional), the solution methods (implicit, explicit) [14–21]. Despite all this, due to the nature of the process, for most of these articles an experimental comparison was not feasible or the experiments realized seemed to be far from industrial cases (i.e. to reduce the computational time the axial rolls are neglected).

In this paper, the authors want to test a new Deform subroutine. This FEM engine is extremely efficient and it was specifically designed for ring rolling. Due to this new subroutine a decrease of the computational time is observed (days instead of weeks). The system utilizes an Arbitrary Lagrangian Eulerian (ALE) solver with automated time stepping. The ALE approach is an attempt to combine the advantages of the Eulerian and Lagrangian formulation methods. In the ALE formulation, a reference system is defined such that co-ordinates are neither fixed in space nor attached to the material. This computational reference system (CRS) is used in conjunction with a second reference system, the material reference system (MRS) which behaves as a Lagrangian mesh. The ALE formulation permits independent mesh movement in the CRS,

which in turn allows the use of a non-uniform mesh with element concentration in the roll gap regions [21]. The model uses hybrid mesh elements and a rigid-plastic finite element method is adopted to improve the computational accuracy. The remeshing strategy is also selected to reduce element distortion and maintain a high quality mesh throughout the simulation. The updating and contact algorithms are optimized for ring rolling. The result is an accurate solution, without artificial constraints on the rotation axis. The ALE solver coupled with the hybrid mesh approach alleviates respectively the difficulties related to the large transformation involved (first factor) and the number of elements needful (second factor); despite this up to now no significantly improvement is available to reduce the computational time affected by the non-linearity relation of the material flow curves (third factor).

The software, due to self centering properties, lets to simulate the process without the guide rolls. Moreover due to the nature of the process it is possible to reduce the number of elements, and so the computational time, by a symmetric simulation of the process. In Fig. 2 the main mechanical parts involved into the ring rolling modeling are summarized.

## FE results and experimental comparisons

The accuracy of the FE model was tested based on the experimental results acquired at an industrial plant. The experimental values have been evaluated by suitable sensors mounted on a ring rolling machine in order to acquire the growing of the ring (diameter, height and width of the ring) and the roll idle compression force needed to deform it.

**Table 1** Nominal chemical composition (weight %) of AISI 1040 [22]

C	0.370–0.440%
Fe	98.6–99.0%
Mn	0.60–0.90%
P	≤ 0.040%
S	≤ 0.050%

A ring rolling process of a ring with a rectangular cross section was tested. The initial dimensions are 1 m for the external diameter and 0.6 m for the initial height. At the end of the process the ring will increase its diameter of 90% while the final height decreases of about 10%.

For the numerical simulation a medium carbon steel (the same used for the experimental results) AISI 1040 was considered. The chemical composition of the worked material is reported in Table 1.

Because of the bulk dimensions of the work piece and of the time needed to deform it (less than 5 min), the working temperature of the process was set constant and equal to 1,150°C.

The simulation was executed taking into account the following constraints:

- no guide rolls, Deform software provides a symmetric simulation with respect to the origin of the axes that coincides with the centre of the ring, so the ring will always be centred;
- symmetrical simulation of the process referred to the middle section of the ring;
- the driver, axial and idle rolls are assumed as rigid objects;

- initial height ( $H_i$ ) of the simulated ring was set lower than the real one. This constraint is necessary because the first working phase of the industrial ring rolling process is characterized by a loss of materials as oxidized slugs. This implies a loss of volume equal to 2–4%. So the initial and the final volume will be different. Because Deform does not take into account loss of elements, a new approach was followed in order to solve this problem. The numerical initial volume ( $V_i$ ) was set equal to the industrial final one ( $V_f$ ), the initial external ( $D_{ext-in}$ ) and inner ( $D_{int-in}$ ) diameters were set equal to the industrial ones. This implies, for the constancy of volume, that the initial numerical height was set lower than the real one. The initial numerical height was so evaluated according to the following formula:

$$H_i = \frac{4V_i}{\pi(D_{ext-in}^2 - D_{int-in}^2)} \quad (1)$$

- conjugate gradient solver with a direct iteration method;
- shear friction factor equal to 0.7;

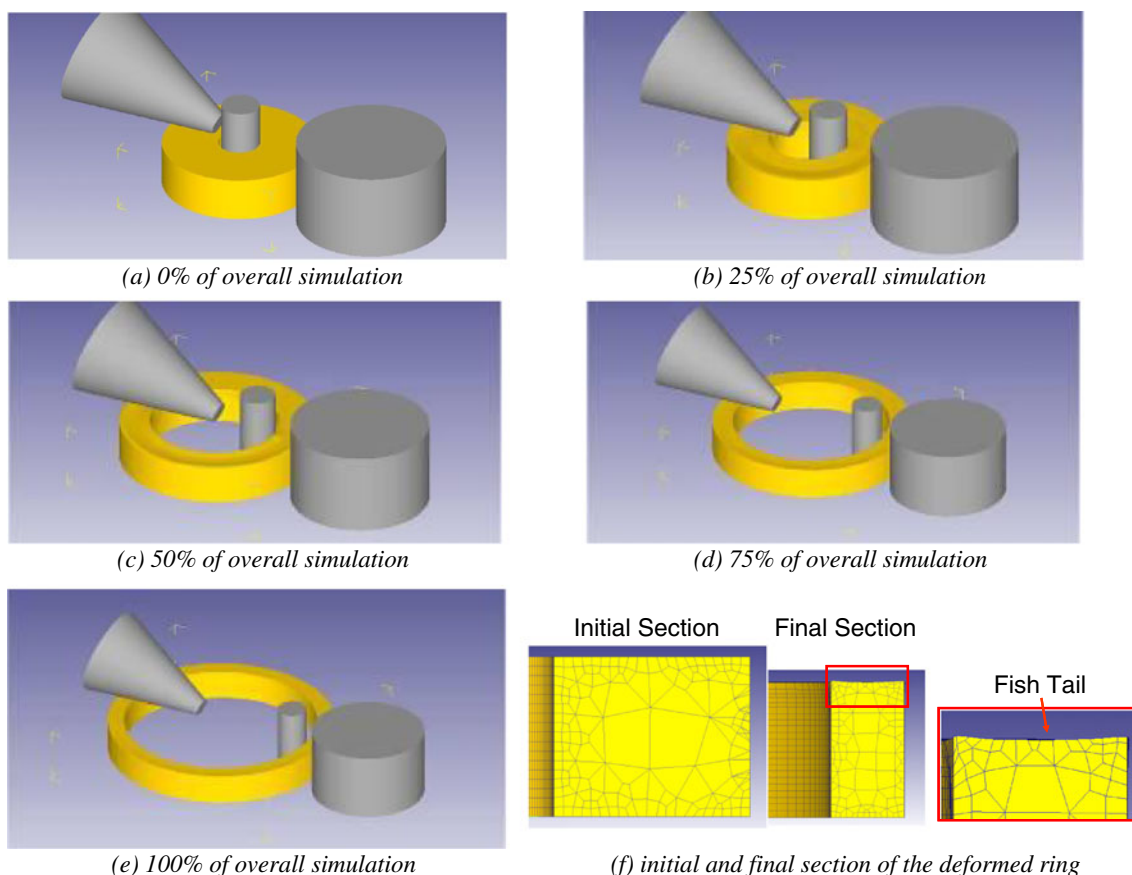
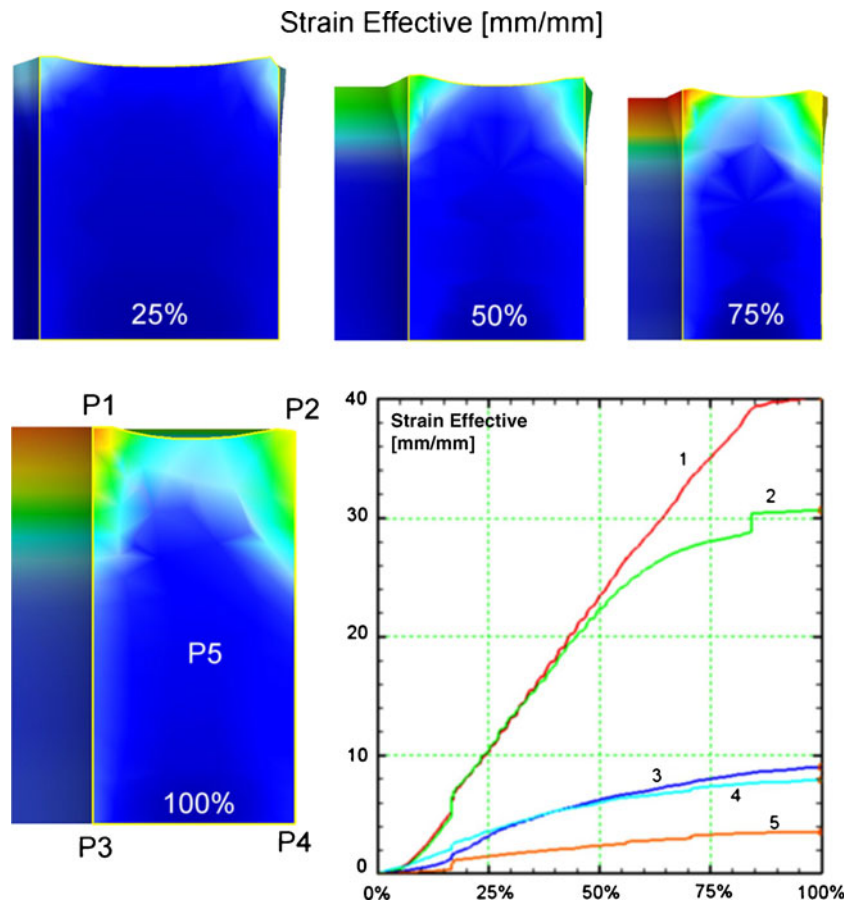


**Fig. 3** 3D-FE model of the ring rolling process. **a** 0% of overall simulation. **b** 25% of overall simulation. **c** 50% of overall simulation. **d** 75% of overall simulation. **e** 100% of overall simulation. **f** initial and final section of the deformed ring

**Fig. 4** Effective strain distributions in the under deformation section for different moment of the process (25%, 50%, 75% and 100% of the total process time) and point tracking plot for 5 points of the section



- the idle roll feed and the axial roll feed were imposed as a function of time. According with the industrial process, a cubic equation was estimated for the idle roll feed. The axial roll feed was subdivided into three steps: stationary, linear and quadratic feed. This choice is due to how it really works on the industrial production. Indeed when the idle roll starts to push the ring towards the driven roll the axial roll doesn't move yet and only deformation of width occurs. After that, the axial roll is rapidly moved by a linear law imposing the height reduction. In the last part of process the height deformation is reduced following a quadratic feed law.

Under the mentioned hypothesis a simulation of a ring rolling process was executed. In Fig. 3 the growing of the ring as a function of the overall simulation time is reported. Figure 3f also shows the initial and final section of the ring. It can be observed that the increasing of the outer diameter is due by an high reduction of the width (60% about) and a low reduction of the height (about 10%). However it must be underlined that the initial height chosen for the numerical model is less than the industrial one for the above mentioned slug problem; indeed the height reduction is equal to 15%. At the end of the simulation the fishtail defect, typical of this type of process, is also achieved.

The use of simulative tools allows to obtain important information on the deformation process of the ring. In fact, as reported in Figs. 4 and 5, it is possible to follow the

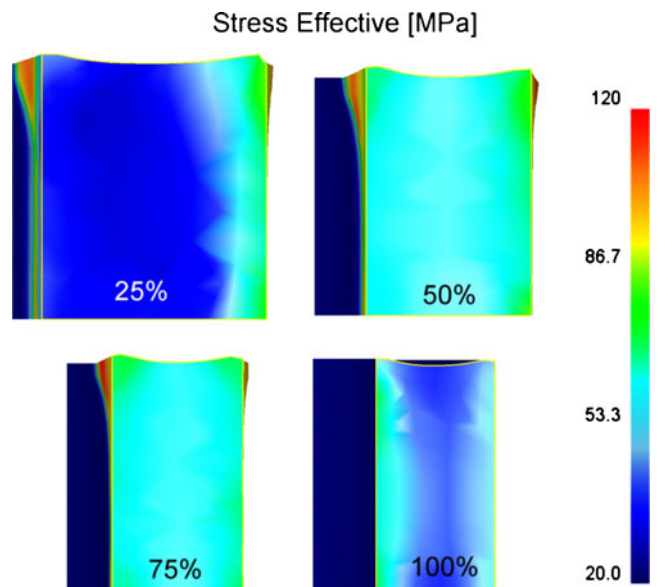


**Fig. 5** Effective stress distributions in the under deformation section for different moment of the process (25%, 50%, 75% and 100% of the total process time)

**Table 2** Point coordinate selected

Point	Coordinate (x,y,z)
P <sub>1</sub>	( $\frac{1}{2} D_{ext-in}$ , 0, 0)
P <sub>2</sub>	( $\frac{1}{2} D_{int-in}$ , 0, 0)
P <sub>3</sub>	( $-\frac{1}{2} D_{ext-in}$ , 0, 0)
P <sub>4</sub>	( $\frac{1}{2} D_{int-in}$ , 0, $H_f/2$ )

deformation and stress history of the material as the rolling process continues at different locations inside the roll section.

Referring to deformations (Fig. 4) it is clear that the material fibres located at the external ring surface (points P1 and P2) are characterized by higher strain, while points P3, P4 and P5 undergo to lower strains (about 25–30% of the strain of points P1 and P2). The high deformations of the outer surface are beneficial for the wear and fatigue resistance of the ring and they can be optimised by changing the process parameters. The results reported in this paper refer to optimised working conditions and the quality of the actual component has found to be good. The sections are realized in correspondence of the drive roll—idle roll area.

Figure 5 illustrates the stress distributions at the contact area between ring and cylinder for different percentages of the total process time (25%, 50%, 75% and 100%). Simulation also helps for this parameter optimization. Moreover, from the knowledge of the stress distribution inside the material it is also possible to carry out a die stress analysis in order to study the pressure and the tangential stresses acting on the rolls in order to forecast their life.

In order to compare the numerical results with the experimental measurements a point tracking was executed. Due to the point tracking function is possible to calculate for each step the geometric position of each node of the meshed ring.

The external diameter ( $D_{ext}$ ), the width of the ring section ( $W$ ) and the ring height ( $H$ ) were selected as the geometrical measures to compare with the experimental

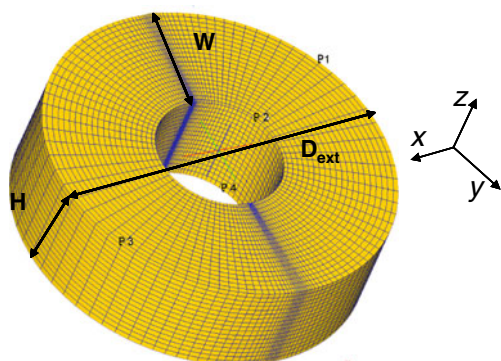


**Fig. 6** Work piece points chosen for the point tracking acquisition

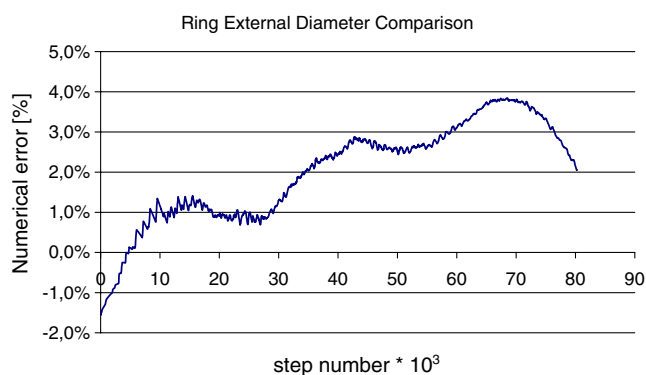


**Fig. 7** Ring external numerical error trend

results. Four nodes (three on the medium section of the ring and one on the upper surface) were selected in order to evaluate the mentioned geometrical values. In Table 2 and Fig. 6 the coordinates and the scheme of these points are respectively reported.

Starting from the results of the point tracking function the mentioned geometrical values ( $D_{out}$ ,  $W$ ,  $H$ ) were evaluated. The comparison between the numerical and the experimental results is reported as a function of the numerical error that is an index described by Eq. (2):

$$Numerical\ error = \frac{Experimental\ value - Numerical\ value}{Experimental\ value} \quad (2)$$

In Figs. 7, 8 and 9 the numerical error trends are reported as function of the step number for the outer diameter, the width and the height of the ring.

As it can be seen the FE model can predict the final dimensions of the ring with a good accuracy (less than 3%) besides the whole numerical error has values lower than 6%. So the numerical results are able to predict the experimental values with a good accuracy also during the whole process. The only exception is related with the first part of the roll height. However it must be taken into account that the initial simulated height of the ring was selected lower than the real one because the software is not

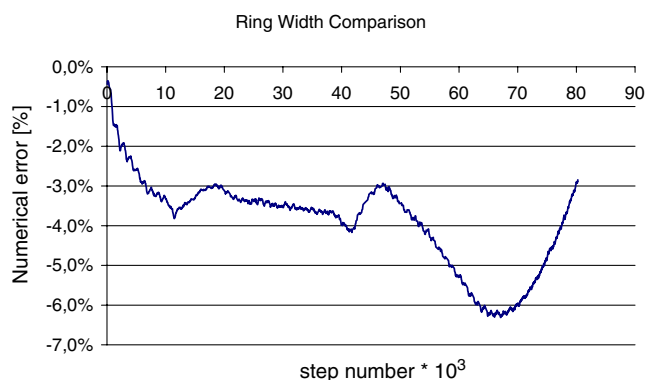


**Fig. 8** Ring width numerical error trend

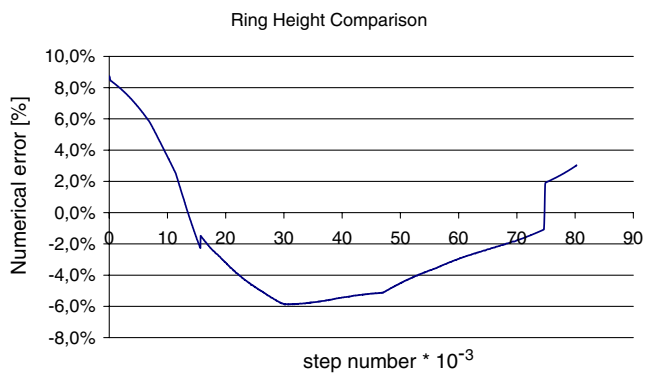


**Fig. 9** Ring height numerical error trend

able to evaluate the loss of material that characterizes the process as above explained.

To execute the physical analysis, the numerical error of the idle roll force was evaluated in order to verify if the simulation was conducted under the same force of the experimental results. In Fig. 10 the numerical error, evaluated following the assumption adopted for the geometrical comparison, is reported. As can be observed the numerical model estimates the idle roll compression force with a numerical error equal to 20% at the beginning and at the end of the process while in the middle the prediction is very accurate ( $\pm 5\%$ ). The reasons of the initial and final deviations from the experimental values are addressed to two different effect: at the beginning of the process the loss of material due to the oxidized slugs affects the measured experimental force while at the end of the process the increasing of the numerical error referred to the width and the external diameter affect the estimation of the idle roll compression force. Besides it must be specified that the acquisition of the experimental values is affected by a considerable noise that justifies the amplitude of the numerical error trend too.

One of the main advantage of the numerical method, once validated, is the computation of different physical parameters that it is difficult to evaluate by experimental approach. As example, to correctly design a ring rolling machine the knowledge of the different loads applied on the

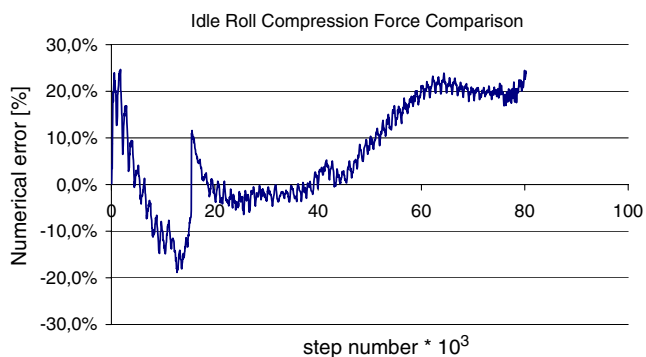


**Fig. 10** Idle roll compression force numerical error trend

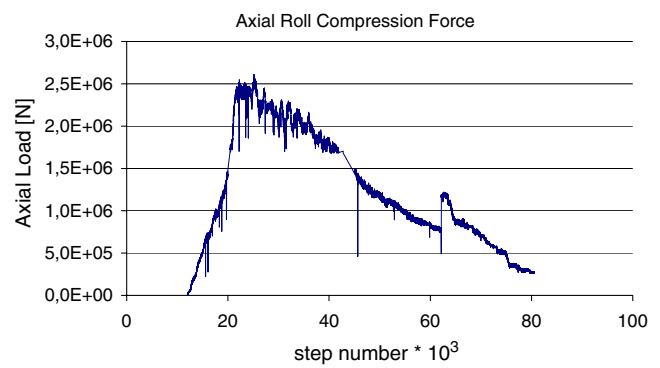


**Fig. 11** Axial roll compression force

rolled ring are needful parameters. In Figs. 11 and 12 the trend of the axial roll force and of the driven roll torque as a function of the simulated step are reported.

As can be observed the two physical variables have similar trend. In the first part of the process there is no contact between axial rolls and the work piece as it also underlined by the Fig. 9; suddenly is observed a high increasing of the load until the maximum value of 2.5 MN after that the load rapidly decrease. By a comparison between the two graphs is possible to understand how the axial rolls affect the value of the driving roll torque. Indeed as can be observed the slope of the torque graph (Fig. 12) increases when the value of the axial load (Fig. 11) starts to become considerable; moreover the maximum value is achieved at the same step increment after which both graphs decrease following a similar slope. For the design and optimization of a ring rolling machine this comparison is very helpful because it underlines which ones are the highest values achieved during the ring deformation and which part of the process is more critical and must be optimized.

## Conclusions

In this paper the effectiveness of a new numerical subroutine was tested by a comparison with experimental

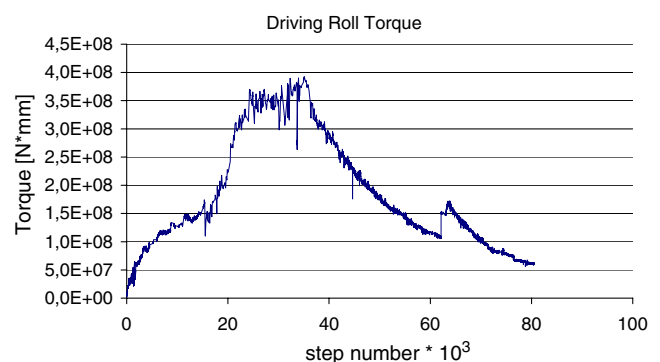


**Fig. 12** Driving roll torque

values acquired from an industrial plant. The results show that the model is able to predict with a good accuracy the final geometric dimensions of the ring. The force used to deform it was also compared and it showed a reasonable result. So it is possible to state that the numerical approach can be used to optimize the process parameters, to evaluate some physical variable difficult to measure and to find, as example, new milling curves able to work the same ring but using less force. Actually more focused researches, based on a numerical approach, are under development investigating about the influence of the initial ring section geometry on the power needed to work it.

## References

1. Shivpuri R, Eruc E (1995) *Int J Mach Tools Manufact* 32:379–398
2. Johnson W, Mamalis AG (1979) *Int Metals Rev* 24:137–148
3. Johnson W, Needham G (1968) *Int J Mech Sci* 10:95–113
4. Johnson W, Macleod I, Needham G (1968) *Int J Mech Sci* 10:455–468
5. Mamalis AG, Johnson W, Hawkyard JB (1976) *J Mech Eng Sci* 18:184–195
6. Utsunomiya H, Saito Y, Shinoda T, Takasu I (2002) *J Mater Process Technol* 125–126:613–618
7. Feng-Lin Y, Lin H, Yong-Qiao W (2007) *Int J Mach Tool Manufact* 47:1695–1701
8. Allwood JM, Kopp R, Michels D, Music O, Öztop M, Stanistreet TF, Tekkaya AE (2005) *CIRP Ann* 54:233–236
9. Li CS, Liu XH, Wang GD (2007) *J Mater Process Tech* 183:425–431
10. Chen JS, Roque C, Pan C, Button ST (1998) *J Mater Process Tech* 80:642–646
11. Chen JS, Wang HP (2000) *Comput Methods Appl Mech Eng* 187:441–468
12. Ryoo JS, Yang DY, Johnson W (1985) *Adv Tech Plast* 2:1292–1298
13. Logura CF, Bramley AN (1987) *Int J Mech Sci* 29:149–157
14. Sawamiphakdi K, Pauskar PM, Jin DQ, Lahoti GD (2002) *Proceedings of 7th ICTP*, 1: 28–31
15. Yang H, Wang M, Guo LG, Sun ZC (2008) *Comput Mater Sci* 44:611–621
16. Lim T, Pillinger I, Hartley P (1998) *J Mater Process Tech* 80–81:199–205
17. Yea Y, Ko Y, Kim N, Lee J (2003) *J Mater Process Technol* 140:478–486
18. Song JL, Dowson AL, Jacobs MH, Brooks J, Beden I (2002) *J Mater Process Tech* 121:332–340
19. Wang M, Yang H, Sun ZC, Guo LG (2009) *J Mater Process Tech* 209:3384–3395
20. Sun Z, Yang H, Ou X (2008) *Trans Nonferrous Met Soc China* 18:1216–1222
21. Davey K, Ward MJ (2002) *J Mater Process Tech* 125–126:619–625
22. Davis JR (1996) *ASM specialty handbook—carbon and alloy steels*